

**Graduate Student Recruitment and Training Support**

**Report for**

**One Ajahn, One Project**

**May 2003 through April 2004**

**Academic Year 2546**

Associate Professor Dr. Kenneth J. Haller  
School of Chemistry  
Institute of Science  
Suranaree University of Technology  
Nakhon Ratchasima 30000

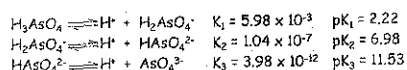
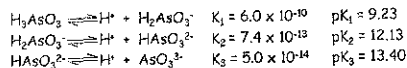
# PHASE DIAGRAM OF BARIUM ARSENATE

Winya Dungkaew and Kenneth J. Haller

## Introduction

Arsenic is a metalloid found in the earth's crust and oceans. Arsenic contamination in the environment, especially in water, results in the transfer of arsenic into living organisms. Arsenic in the human body may affect several organs such as the gastrointestinal tract, respiratory tract, skin, and liver<sup>1</sup>. Arsenic can occur in the environment in several oxidation states (-3, 0, +3, +5) but in natural waters is mostly found as arsenic(III) and arsenic(V).

The speciation of arsenic depends on pH and potential as shown in the Eh-pH diagram<sup>2</sup> (Figure 1) and speciation vs pH diagram calculated from  $pK_a$ 's (Figure 2). The dissociation reactions and dissociation constants at 25 °C<sup>4</sup> of arsenous acid and arsenic acid are:



Pookrod, Haller & Scamehorn<sup>5</sup> have demonstrated that polyelectrolyte enhanced ultrafiltration (PEUF) can achieve 99.95% removal of arsenate anion from solutions with starting arsenic concentrations of 100 µg/L. To make the process economical the polyelectrolyte must be recovered for reuse in the process. The recovery process is based on precipitation (crystallization) of arsenate anion from polyelectrolyte-arsenate complexes to regenerate the polyelectrolyte. Divalent metal cations such as barium(II) should be ideal candidates for this regeneration due to their very low Ksp values with arsenate anion which should lead to stable solid phase products.

This work reports study of the relationship of the solid phase barium and arsenate compounds versus concentration (molar ratio of barium/arsenate) and pH in a phase diagram. This diagram is useful to predict which species (phase) will be formed at a given concentration and pH, and thus to aid the understanding of the barium(II) cation/arsenate(III) anion system behavior.

## Experimental

The preparation of barium arsenate compounds for 1:2 barium/arsenate molar ratio was carried out in glass bottle by mixing 10 mL of 0.04 M of barium solution (2.0 mL of 0.2 M analytical grade BaCl<sub>2</sub>·2H<sub>2</sub>O solution diluted to 10 mL with distilled water and pH adjusted to 2.0-12.0 by HCl or NaOH solution) with 10 mL of 0.08 M arsenate solution (1.6 mL of 0.5 M analytical grade Na<sub>2</sub>HAsO<sub>4</sub>·7H<sub>2</sub>O solution diluted to 10 mL with distilled water and pH adjusted by HCl or NaOH solution), giving 20 mL total volume of 0.04 M arsenate and 0.02 M barium solution. After mixing, the pH of solution was measured immediately. The solutions were allowed to stand for 24 hours at room temperature to reach equilibrium, and the pH of the supernatant was measured. The formed solid was separated from the supernatant by filtration with filter paper, and air dried at room temperature. Other barium/arsenate molar ratios (1:1, 3:2, 2:1, 5:2, and 3:1) were prepared by the same procedure except the barium concentration was adjusted to the desired ratio.

The barium arsenate compounds were characterized by powder x-ray diffraction (XRD) using a Bruker axis model D5005 x-ray diffractometer (CuKα radiation, 40 kV and 35 mA, scan range 5.0-70.0° (2θ), scan speed 0.1 sec/step). The diffractograms were compared to the JCPDS (joint committee on powder diffraction standards) files for solid phase identification. Infrared spectra were recorded on a Biorad model FTS175C FTIR for the region 400-4000 cm<sup>-1</sup> (KBr technique). A scanning electron microscope with energy dispersive x-ray fluorescence (JSM-6400 SEM and Microspec model WDX-100 EDX) were used to examine morphology and determine heavy element composition.

## Results and Discussion

The precipitation experiments showed no precipitate formed at pH lower than 5.5; above this pH white precipitates were formed. The results from XRD analysis (Figure 3) shows three pure species of barium hydrogen arsenate monohydrate (BaHAsO<sub>4</sub>·H<sub>2</sub>O), sodium barium arsenate nonahydrate (NaBaAsO<sub>4</sub>·9H<sub>2</sub>O), and barium chloride arsenate (Ba<sub>5</sub>Cl(AsO<sub>4</sub>)<sub>3</sub>) as well as three mixtures of BaHAsO<sub>4</sub>·H<sub>2</sub>O/NaBaAsO<sub>4</sub>·9H<sub>2</sub>O, BaHAsO<sub>4</sub>·H<sub>2</sub>O/Ba<sub>5</sub>Cl(AsO<sub>4</sub>)<sub>3</sub>, and NaBaAsO<sub>4</sub>·9H<sub>2</sub>O/Ba<sub>5</sub>Cl(AsO<sub>4</sub>)<sub>3</sub> found in different concentration and pH regions as shown in the barium arsenate phase diagram (Figure 4). The formation of different species of barium arsenate at different concentration and pH as shown in the phase diagram corresponds to the speciation of arsenic versus pH (Figure 2), at very low pH the solution species is the neutral H<sub>2</sub>AsO<sub>4</sub>. From pH = 2.0-6.5 H<sub>2</sub>AsO<sub>4</sub> is the dominant solution species. Both of these are quite soluble in the presence of Ba<sup>2+</sup> and no barium arsenate precipitate formed at pH lower than 5.0 in the phase diagram. HAsO<sub>4</sub><sup>2-</sup> is the dominant species in the pH range 7.0-11.5, and an important species in the ranges 5.0-7.0 and 11.5-14.0. Thus, in the barium arsenate phase diagram, BaHAsO<sub>4</sub>·H<sub>2</sub>O was found as a dominant species at pH higher than 5.5 to about 11.5 and found as part of a mixture at pH higher than 11.5. At pH higher than 11.5 the dominant solution species is AsO<sub>4</sub><sup>3-</sup>, but again it also can exist at pH lower than 11.5, resulting in NaBaAsO<sub>4</sub>·9H<sub>2</sub>O in pH range 10.5-12.0 and Ba<sub>5</sub>Cl(AsO<sub>4</sub>)<sub>3</sub> at pH higher than 11.5.

FTIR spectra of the three pure phase are given in Figure 5. BaHAsO<sub>4</sub>·H<sub>2</sub>O, spectrum A, shows a dominant band for As-O asymmetric stretching 877 cm<sup>-1</sup>, and As-OH and As-O symmetric stretching at 691 cm<sup>-1</sup> and 854 cm<sup>-1</sup>, respectively. In Ba<sub>5</sub>Cl(AsO<sub>4</sub>)<sub>3</sub>, spectrum C, the asymmetric stretch is at 812 cm<sup>-1</sup> and the symmetric stretch is at 841 cm<sup>-1</sup>. In NaBaAsO<sub>4</sub>·9H<sub>2</sub>O the symmetric stretch is at 813 cm<sup>-1</sup>. The vibration bands in these samples are shifted from the values found in aqueous arsenic acid<sup>6</sup> where the As-O asymmetric stretching, As-OH and As-O symmetric stretching for HAsO<sub>4</sub><sup>2-</sup> are 865 cm<sup>-1</sup>, 680-700 cm<sup>-1</sup>, and 846 cm<sup>-1</sup>, respectively, and for AsO<sub>4</sub><sup>3-</sup> where the asymmetric stretching is 794 cm<sup>-1</sup> and the symmetric stretching is 814 cm<sup>-1</sup>. The shift of vibration bands of arsenate may be caused by environmental differences of arsenate molecules bound in different crystal forms, which may change the symmetry of arsenate as well as the strength of arsenic-oxygen bonds, leading to shifts in the vibration bands.

The SEM micrograph patterns (Figure 6) show the different shapes of each pure phase and the mixture of different particle shapes in the mixed phases. Results from EDX analysis confirm the existence of sodium, barium and arsenic in NaBaAsO<sub>4</sub>·9H<sub>2</sub>O, chlorine, barium and arsenic in Ba<sub>5</sub>Cl(AsO<sub>4</sub>)<sub>3</sub>, and only barium and arsenic in BaHAsO<sub>4</sub>·H<sub>2</sub>O.

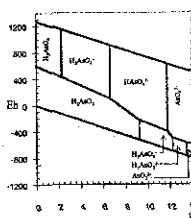


Figure 1. Eh-pH diagram for arsenous and arsenic acid

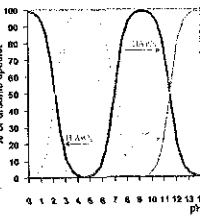


Figure 2. Speciation vs pH diagram for arsenous and arsenic acid

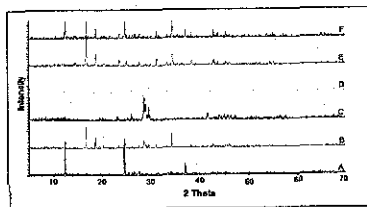


Figure 3. XRD spectra of BaHAsO<sub>4</sub>·H<sub>2</sub>O (A), Ba<sub>5</sub>Cl(AsO<sub>4</sub>)<sub>3</sub> (B), NaBaAsO<sub>4</sub>·9H<sub>2</sub>O (C), NaBaAsO<sub>4</sub>·9H<sub>2</sub>O + BaHAsO<sub>4</sub>·H<sub>2</sub>O (D), NaBaAsO<sub>4</sub>·9H<sub>2</sub>O + Ba<sub>5</sub>Cl(AsO<sub>4</sub>)<sub>3</sub> (E) and BaHAsO<sub>4</sub>·H<sub>2</sub>O + Ba<sub>5</sub>Cl(AsO<sub>4</sub>)<sub>3</sub> (F)

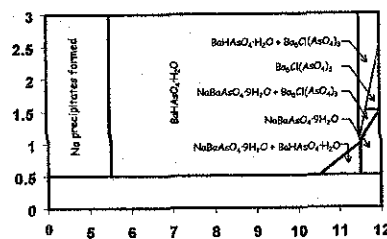


Figure 4. Barium arsenate phase diagram

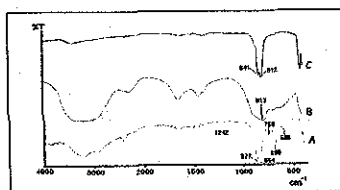


Figure 5. FTIR spectra of BaHAsO<sub>4</sub>·H<sub>2</sub>O (A), NaBaAsO<sub>4</sub>·9H<sub>2</sub>O (B), Ba<sub>5</sub>Cl(AsO<sub>4</sub>)<sub>3</sub> (C)

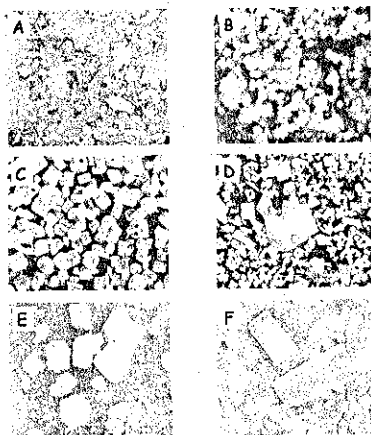


Figure 6. SEM micrograph of BaHAsO<sub>4</sub>·H<sub>2</sub>O (A), Ba<sub>5</sub>Cl(AsO<sub>4</sub>)<sub>3</sub> (B), NaBaAsO<sub>4</sub>·9H<sub>2</sub>O (C), NaBaAsO<sub>4</sub>·9H<sub>2</sub>O + BaHAsO<sub>4</sub>·H<sub>2</sub>O (D), NaBaAsO<sub>4</sub>·9H<sub>2</sub>O + Ba<sub>5</sub>Cl(AsO<sub>4</sub>)<sub>3</sub> (E) and BaHAsO<sub>4</sub>·H<sub>2</sub>O + Ba<sub>5</sub>Cl(AsO<sub>4</sub>)<sub>3</sub> (F)

## References

- Mandal, B. K. & Suzuki, K. T. (2002). *Talanta*, 58, 201-235.
- Drawn after Brookins, D. G., Springer-Verlag: Berlin, 1988.
- <http://jchemed.chem.wisc.edu/JCEWWW/Features/WebWare/wweg4/sheets/alphawex.xls>
- National Research Council (U.S.). (1999) Subcommittee on Arsenic in Drinking Water, National Academy Press: Washington DC, 330.
- Pookrod, P.; Haller, K. J.; Scamehorn, J. F. (2003). *Sep. Sci. Tech.*, accepted for publication.
- Myneni, S. C.; Traina, S. J.; Waychunas, G. A.; Logan, T. J. (1998). *Geochemica et Cosmochimica Acta*, 62, 3499-3514.

## Acknowledgements

- Thailand Research Fund (TRF) under the Royal Golden Jubilee PhD Scholarship Program (3.C.TS/44/B.1)
- Suranaree University of Technology (SUT) for a travel grant to attend this meeting.